RIP140 increases APC expression and controls intestinal homeostasis and tumorigenesis.

Marion Lapierre, Sandrine Bonnet, Caroline Bascoul-Mollevi, Imade Ait-Arsa, Stéphan Jalaguier, Maguy del Rio, Michela Plateroti, Paul Roepman, Marc Ychou, Julie Pannequin, et al.

RIP140 increases *APC* gene expression and controls intestinal homeostasis and tumorigenesis

Marion LAPIERRE[1], Sandrine BONNET[1], Caroline BASCOUL-MOLLEVI[2], Imade AIT-ARSA[1], Stéphan JALAGUIER[1], Maguy Del RIO[1], Michela PLATEROTI[3], Paul ROEPMAN[4], Marc YCHOU[5], Julie PANNEQUIN[6], Frédéric HOLLANDE[6], Malcolm PARKER[7] and Vincent CAVAILLES[1]

[1] IRCM, Institut de Recherche en Cancérologie de Montpellier, INSERM U896, Université Montpellier 1, Montpellier F-34298, France; [2] CRLC Val d'Aurelle Paul Lamarque, Unité de Biostatistique, Montpellier F-34298, France; [3] Centre de Génétique et de Physiologie Moléculaire et Cellulaire, Université Lyon 1, CNRS, Villeurbanne F-69200, France; [4] Agendia NV, Amsterdam, the Netherlands, and Agendia Inc, Irvine, CA; [5] CRLC Val d'Aurelle Paul Lamarque, Service d'Oncologie Digestive, Montpellier F-34298, France; [6] Centre National de la Recherche Scientifique (CNRS), Unité Mixte de Recherche (UMR) 5203, Institut de Génomique Fonctionnelle, F-34000 Montpellier, France; [7] Institute of Reproductive and Developmental Biology, Faculty of Medicine, Imperial College London, United Kingdom.

Contact: Dr Vincent Cavaillès, IRCM - INSERM U896, 208 rue des Apothicaires, Montpellier F-34298, France. E-mail: vincent.cavailles@inserm.fr

Phone: 33 4 67 61 24 05. Fax: 33 4 67 61 67 87

Running title: RIP140 in colon cancer

Total length: 9885 words

Conflict of interest: None

ABSTRACT

Deregulation of the Wnt/APC/β-catenin signaling is an important consequence of the *APC* tumor suppressor gene dysfunction. Genetic and molecular data have established the importance of this pathway in the development of colorectal cancer. Here, we demonstrate that RIP140, a transcriptional coregulator, regulates intestinal homeostasis and tumorigenesis. Using loss and gain of function mouse models, we show that RIP140 inhibits the proliferation and apoptosis of intestinal epithelial cells. Interestingly, the same effect of RIP140 was observed on cell proliferation in the intestinal epithelium following mice whole body irradiation. RIP140 also strongly represses human colon cancer cell proliferation in vitro and in vivo after grafting onto nude mice. Moreover, both in mice tissues and in human cancer cells, RIP140 stimulates *Apc* gene transcription and inhibits β-catenin activation and target gene expression. Finally, RIP140 mRNA and protein levels are lower in human colon cancers than in normal mucosa and low RIP140 expression is correlated with poor survival. Altogether, these results support a tumor suppressor role for RIP140 in colon cancer.

165/200 words

INTRODUCTION

The Wnt pathway is one of the major pathways deregulated in colorectal cancer. In the normal physiological gut, activation of this pathway ensures the proliferation of precursor cells and the renewal of the intestinal epithelium by activating the transcriptional properties of the T cell factor/lymphoid enhancer factor-1 family (1). Stimulation by Wnt ligands leads to the stabilization of the transcription co-activator β-catenin, which becomes associated with TCFs in the nucleus, leading to the expression of specific target genes. Canonical Wnt signaling operates by regulating the phosphorylation and degradation of β-catenin (2). Without stimulation by Wnt ligands, the levels of β-catenin in the cytoplasm are normally regulated by a multiprotein destruction complex that targets for degradation. This complex is assembled over the scaffold component Axin which contains binding domains for β-catenin, the tumor suppressor adenomatous polyposis coli (APC) and glycogen synthase kinase-3 (GSK3) and casein kinase 1 (CSNK1). Within the Axin complex, β-catenin is sequentially phosphorylated by CSNK1 and GSK3 and then degraded by the proteasome (3). Thereby, this complex controls the proliferation of intestinal epithelial cells by maintaining the pool of active β-catenin. However, mutations of the *APC* gene, which were first identified in patients suffering from familial adenomatous polyposis (FAP), occur in a high proportion of sporadic colorectal carcinomas (up to 80%) (4). Stimulation of the Wnt pathway due to a mutation in the negative regulator APC provokes the hyperproliferation of the epithelium. Several mouse models have been generated and for instance, the $Apc^{\Delta 14/+}$ mice in which exon 14 has been deleted (frameshift mutation at codon 580) present a FAP phenotype with tumors in the distal colon and rectum, showing that heterozygous disruption of the *Apc* gene

was associated with the accumulation of β-catenin and overexpression of the β-catenin target genes : *Cyclin D1* and *c-Myc* (5).

The transcription cofactor RIP140 (receptor interacting protein, 140 kDa), also known as NRIP1 (nuclear receptor-interacting protein 1), was first identified in human cancer cells through its interaction with estrogen receptor α (6). RIP140 was also shown to interact with many other nuclear receptors and transcription factors (for a review see (7)). More recently, we demonstrated that RIP140 also behaves as an Rb-like regulator of the E2F pathway by directly binding to E2Fs and repressing their transactivation potentials (8). RIP140 mainly acts as a transcriptional repressor by means of four inhibitory domains that recruit histone deacetylases or C-terminal binding proteins (9). Several post-translational modifications, such as sumoylation and acetylation, also play important roles in controlling the subcellular location and repressive activity of RIP140 (for a review (10)). *RIP140* is a ubiquitously expressed gene whose transcription is finely regulated at the transcriptional levels both by nuclear receptors and E2Fs (11). The physiological importance of RIP140 has been evaluated using mice that lack the *Rip140* gene (RIPKO mice). These animals are viable but display a wide range of phenotypic alterations in various tissues and organs such as infertility of female mice (12) or reduced body fat content (13), and, more recently, severe cognitive impairments (14) and mammary gland morphogenesis (15).

Our present results demonstrate the role of RIP140 in homeostasis and tumorigenesis of the intestinal epithelium. We used mice with a loss or gain of RIP140 function to show that RIP140 inhibits cell proliferation and apoptosis in the

intestinal epithelium. At the molecular level, RIP140 positively controls *APC* gene expression and, consequently, reduces β-catenin activation and Wnt target gene expression. The overexpression of RIP140 inhibits the proliferation of human colon cancer cells in vitro and in vivo after grafting onto nude mice. Finally, *RIP140* mRNA and protein levels are reduced in colon cancer biopsies as compared to normal tissue, and tumors with a high RIP140 gene expression specify patients with the best survival rates. Altogether, this work identifies RIP140 as a new key factor regulating intestinal tumorigenesis and as a potential new biomarker in oncology.

RESULTS

RIP140 expression in the intestinal epithelium

Previous data indicated that RIP140 is a ubiquitously expressed transcription factor (16). By RT-qPCR analysis, the *Rip140* (*Nrip1*) mRNA was detected in all the mouse tissues tested and particularly, in the intestine and colon (Supplementary Figure 1A). We first analyzed the distribution of RIP140 in the intestinal epithelium of wild-type mice by immunofluorescence. We found that RIP140 was expressed in the nucleus of all epithelial intestinal cells, with a clearly increasing gradient along the crypt-villus axis (Figure 1A). To confirm this observation, we applied sequential isolation of wild-type mouse small intestinal epithelial cells. To verify the enrichment of the different fractions in villus-associated or crypt-associated cells, we quantified the mRNA levels of the *Lysozyme* (*Lyz)* and *Mucin 2* (*Muc2*) genes, which are respectively differentiation markers of Paneth cells located in the crypts and goblet cells in the villi (17). As expected, the *Lyz* gene was exclusively expressed in cells from fraction 4 whereas the *Muc2* gene was mainly expressed in cells from fractions 1 and 2 (Figure 1B). Using the same enriched fractions, we found that the expression of *Rip140* mRNA was significantly higher in differentiated cells of the villi than in cells from the crypts (Figure 1B).

RIP140 alters small intestine homeostasis

To study the role of RIP140 in the intestinal epithelium, we used *Rip140* null (*RIPKO*) or *RIP140* transgenic (*RIPTg*) mice. In these two mouse models, the respective deletion and overexpression of the *Rip140* gene in intestinal sections were validated by immunofluorescence (Supplementary Figure 1B). As expected, the RIP140 protein

was undetectable in the *RIPKO* mice and overexpressed in the nuclei of all intestinal epithelial cells in the *RIPTg* mice as compared to their wild-type littermates. RT-qPCR analysis confirmed that *RIPKO* mice expressed β-galactosidase as a marker of the mouse *Rip140* gene disruption (12) and that the transgenic human *RIP140* gene was specifically expressed in *RIPTg* mice (Supplementary Figure 1C).

Qualitative histopathological analysis of paraffin sections stained with hematoxylin and eosin demonstrated no gross morphological changes in the structures of the intestinal epithelia of the two mouse models (Figure 1C, left panel). However, precise measurements of villus and crypt lengths demonstrated statistically significant differences between transgenic and wild-type animals (Figure 1C, right panel). Indeed, when compared to wild-type animals, the length of the crypt-villus axis increased in *Rip140* null mice and decreased in mice overexpressing RIP140. This was associated with an altered total length of the small intestine which was shorter in RIPKO mice and longer in *RIPTg* animals when compared to their respective wild-type littermates (Supplementary Figure 1D, top panel). As a consequence, invalidation or overexpression of the *Rip140* gene did not affect the total surface area of the intestinal epithelium (Supplementary Figure 1D, bottom panel).

RIP140 inhibits cell proliferation and apoptosis

To determine whether cell proliferation was regulated by RIP140 expression, mice were injected with 5-ethynyl-2'-deoxyuridine (EdU) 2 hours prior sacrifice. As shown in Figure 2A, the analysis of EdU labeling demonstrated that the number of cells synthesizing DNA was significantly increased (2.6-fold) in *RIPKO* mice as compared to wild-type animals. By contrast, the level of EdU staining decreased (3.7-fold) in *RIPTg* mice as compared to control mice. These results were strengthened by

quantifying the mRNAs corresponding to *Myc* and *Pcna* (proliferating cell nuclear antigen) genes (Supplementary Figure 2A). The corresponding mRNA levels were increased up to 2-fold in *RIPKO* mice and decreased by up to 3-fold in the RIPTg strain as compared to wild-type animals. The differences in the expression of the *Pcna* gene among the three genotypes were confirmed by immunofluorescence labeling (Supplementary Figure 2B). We next assessed the effect of RIP140 expression on apoptosis by TUNEL assay on intestinal sections. The top of the villi showed a significant 3-fold increase in TUNEL-positive cells in *Rip140* null mice as compared to wild-type littermates, whereas villi overexpressing RIP140 (RIPTg) showed a clear 2-fold decrease in apoptosis (Figure 2B). Altogether, these observations suggest that RIP140 regulates both cell proliferation and apoptosis and may therefore inhibit the renewal of the intestinal epithelium.

RIP140 inhibits the response of the intestinal epithelium to irradiation

To highlight the role of RIP140 in the homeostasis of the intestinal mucosa, *RIPKO* and *RIPTg* mice together with their wild-type littermates were exposed to a single 12 Gy whole body irradiation (WBI). At day 2.5, a time when recovery is initiated, we assessed the number and length of villi, together with the length of crypts after hematoxylin-eosin staining of intestinal paraffin sections (Figure 2C). Following WBI, *Rip140* null mice exhibited a significant increase number of regenerating villi as compared to wild-type animals. The length of villi and crypts was also significantly higher in RIPKO animals. As shown in Supplementary Figure 2C, this effect was associated with a strong rise in PCNA staining in the crypts where progenitors and stem cells reside and suggested a role for RIP140 in ionizing radiation-induced cell proliferation. As expected, this process was much slower in *RIPTg* mice (Figure 2C)

which exhibited only few buds of villi and weak PCNA staining of crypt cells 2.5 days after WBI (Supplementary Figure 2C). Altogether, these results strongly indicate that RIP140 inhibits the renewal of the intestinal epithelium.

RIP140 controls β-catenin activation

The Wnt/APC/β-catenin signaling is the major pathway regulating cellular homeostasis of the intestinal epithelium (18). To decipher the underlying mechanisms involved in the effect of RIP140 in intestinal epithelium homeostasis, we sought to establish whether its expression impacted the Wnt/APC/β-catenin signaling pathway. We first investigated the pattern of β-catenin expression and activity in the intestinal epithelia of the different mutant mice (Figure 3A). Immunolabeling of paraffin sections of small intestine from *Rip140* null and transgenic mice revealed no significant differences in the levels of total β-catenin (Figure 3A, left panel). We then measured the level of active β-catenin (which represents only a small fraction of total β-catenin (19)) using a specific antibody for the protein dephosphorylated on Ser37 or Thr41. Quantification of active β-catenin (ABC) staining revealed a clear regulation by RIP140 with an increase by 2-fold in *RIPKO* mice and a decrease by about 3-fold in *RIPTg* mice as compared to controls (Figure 3A, right panel). In order to validate the regulation of β-catenin activation by RIP140, we evaluated β-catenin transcriptional activity in intestinal epithelium by quantifying the mRNA levels of several target genes. As shown in Figure 3B, we observed a significant regulation of most of these genes (for instance *c-Myc*, *Claudin-1* (20), *Endothelin-1* (21), *Jagged-1* (22) and *c-Jun* (23)) whose mRNA levels were increased in *Rip140* null mice and reduced in *RIPTg* mice as compared to wild-type animals. For Endothelin-1 and Jagged-1, the same deregulation was observed at the protein level by immunofluorescence (data

not shown). Finally, since activation of the Wnt pathway drives the differentiation program of Paneth cells (24), we investigated the effect of RIP140 on this lineage. Using a specific antibody directed against lysozyme, we observed that the number of Paneth cells per crypt increased in *RIPKO* mice and decreased in *RIPTg* (Supplementary Figure 3), thus strengthening the negative regulation of the Wnt signaling pathway by RIP140.

RIP140 positively regulates *Apc* gene expression

The levels of active β-catenin is normally controlled by a multiprotein degradation complex composed of APC, AXIN1 and 2, GSK3β, CSNK1 and PP2A (18). We therefore postulated that RIP140 could control the level of β-catenin activation by influencing the expression of members of this degradation complex. To test this hypothesis, we quantified the mRNAs encoded by the main genes implicated in β-catenin degradation. Interestingly, we found a correlation between the expression of the *Rip140* gene and the mRNA levels of *Apc, Axin2* and *Csk1E* genes which were decreased and increased in *Rip140* null and transgenic mice, respectively (Figure 3C). This suggests that RIP140 inhibits β-catenin activation in the intestinal epithelium by positively regulating the expression of several members of the β-catenin degradation complex. Altogether, this inhibition of the β-catenin signaling pathway could explain, at least in part, the above-described effects of RIP140 on intestinal homeostasis.

RIP140 inhibits proliferation of human colon cancer cells

Given the critical role played by the Wnt/APC/β-catenin pathway in promoting colon tumorigenesis, we then investigated the role of RIP140 in human colon cancer cells.

We first measured the expression of the *RIP140* gene in different colorectal cancer cell lines by RT-qPCR and observed that the gene was much more weakly expressed in colon cancer cells than in breast cancer cell lines (data not shown). To analyze the effects of RIP140 on the malignant phenotype of human colon adenocarcinoma cells, we established a stably transfected HCT116 cell line overexpressing a GFP-tagged version of RIP140 (HCT-RIP cells) and used as a control the same cells transfected with the pEGFP empty vector (HCT-GFP cells). Real-time qPCR analysis confirmed the much greater abundance of RIP140 mRNA in the HCT-RIP cells compared to control HCT-GFP cells (Figure 4A, left panel). Similarly, western blotting analysis confirmed that the GFP-RIP140 protein was overexpressed in the nuclear fraction of HCT-RIP cell lysates (Figure 4A, right panel). Fluorescence analysis of HCT-GFP and HCT-RIP cells revealed a cytoplasmic labeling corresponding to GFP expressing cells and, as expected, a punctuate signal corresponding to the previously described localization of the GFP-RIP140 protein in speckles (25) (Figure 4A, right panel).

We first investigated the effect of RIP140 expression on cell proliferation using the XCELLigence technology (Roche Diagnostics) which allows real-time monitoring of cell proliferation through measurement of impedance-based signals. Data shown in Figure 4B clearly demonstrated that RIP140 inhibited human colon cancer cell proliferation in vitro. To determine whether RIP140 affected cell cycle progression, we transiently transfected the two stable HCT116 cell lines with a cdt1-RFP Premo™ FUCCI Cell Cycle Sensor allowing the detection of cells in G1. In parallel, we performed EdU labeling in order to monitor cells synthesizing DNA (Figure 4C). When compared to control cells, HCT-RIP cells showed a strong and significant decrease in the S-phase cell population (from 43.8% to 17.8%) with a concomitant increase in the number of cells in the G1 phase (from 24.1% to 34.6%). These data

indicated that RIP140 expression resulted in a significant and specific blockade of cell cycle progression with a cell arrest in G1.

We then assessed the impact of RIP140 on tumor growth in vivo by testing the ability of HCT-GFP and HCT-RIP cells grafted subcutaneously onto immunodeficient mice to form tumors (Figure 4D). In line with the inhibition of cell cycle progression by RIP140, we observed that tumors from RIP140 overexpressing HCT116 cells exhibited a strong and significant decrease in volume (2.5-fold) as compared to controls (Figure 4D). Sections of HCT-RIP xenografts stained with hematoxylin and eosin showed large areas with faint eosin staining and lysed nuclei which are usually associated with necrosis (Figure 4E). Such areas with karyolysis were significantly smaller in HCT-GFP tumors than in HCT-RIP tumors (14.4 % +/- 8.1 and 45.6 % +/- 19.1 of the whole tumor surface, respectively). Altogether, these data demonstrate that RIP140 inhibits colon cancer cell proliferation in vitro and tumor growth in vivo.

Effect of RIP140 on the Wnt signaling in human colon cancer cells

To investigate whether the effect of RIP140 on human colon cancer cell proliferation was associated with an inhibition of β-catenin activation, we performed immunofluorescence detection of total and active (ABC) β-catenin in the two HCT116 cell lines, overexpressing or not RIP140. As noticed in mouse intestine, we observed no differences in the quantification of total β-catenin immunolabeling (Figure 5A left panel) but measured a 3-fold reduction of ABC staining in cells overexpressing RIP140 (Figure 5A right panel). As shown in Figure 5B, the regulation of dephosphorylated β-catenin expression by RIP140 was confirmed by western-blot experiments. As observed in mouse intestinal epithelium, this effect was associated with a decrease of several β-catenin target genes in HCT-RIP cells (Figure 5C). To

demonstrate more directly the regulation of the Wnt pathway by RIP140, we performed the classical TCF reporter assay by transiently transfecting the two reporter plasmids (pTOPflash or pFOPflash) into our stable HCT116 clones overexpressing or not RIP140. As shown in Figure 5D (left panel), the level of β-catenin-driven transcription activity measured as the TOP/FOP luciferase reporter ratio was significantly lower in RIP140 overexpressing HCT116 cells (HCT-RIP) as compared to control HCT116 cells (HCT-GFP). Finally and as expected, an up-regulation of the same Wnt reporter assays was noticed in mouse embryonic fibroblasts isolated from *RIPKO* embryos as compared to wild-type MEFs (Figure 5D right panel). In order to strengthen these data, we then analyzed the effect of siRNA-mediated depletion of RIP140 expression in human colon cancer cells. To this end, we used RKO colon cancer cells which exhibit an intact Wnt/APC/β-catenin pathway. Interestingly, the knock-down of RIP140 expression in RKO cells (RKO-siRIP vs RKO-siCTL cells - Supplementary Figure 4A) led to an increase of active β-catenin staining (Supplementary Figure 4B) resulting in an increase of its target gene expression (Supplementary Figure 4C).

Altogether, these results demonstrated a clear inhibition of the Wnt/APC/β-catenin signaling pathway by RIP140. As shown in Supplementary Figure 4D, the impact of RIP140 has been assessed on twelve Wnt target genes both in mouse gut and in human colon cancer cells, a majority of these genes (more than 60% and 80%, respectively) being regulated by RIP140.

RIP140 increases transcription of the *APC* gene in human colon cancer cells

We then quantified the expression of members of the β-catenin degradation complex in the stable HCT116 clones overexpressing or not RIP140. As shown in Figure 6A,

we found that the level of the *APC* tumor suppressor gene was significantly up-regulated about 2-fold in HCT116 cells overexpressing RIP140. The specific deregulation of APC mRNA levels (2-fold decrease) was also observed after siRNA-mediated depletion of RIP140 expression in RKO cells (Figure 6B). Very few studies have examined the regulation of *APC* gene transcription. However, characterization of the proximal promoter region of the human *APC* gene identified functional consensus binding sites for several transcription factors including p53, USF1/2 and Sp1 ((26)(27) and Figure 6C). In order to demonstrate the transcriptional regulation of the *APC* gene by RIP140, we transiently transfected HCT116 colon cancer cells with two reporter constructs containing the *APC* gene proximal promoter region (encompassing sequences of 972bp and 186bp, respectively) fused to the luciferase coding sequence. As shown in Figure 6C, we observed a clear induction of luciferase activity upon cotransfection with a RIP140 expression vector, indicating that RIP140 was able to transactivate the *APC* gene promoter. This effect was specific since control reporter vectors used in parallel were not affected by RIP140 overexpression (Figure 6C and (28)).

Chromatin immunoprecipitation (ChIP) experiments were set up to demonstrate the presence of RIP140 on the proximal region of the *APC* promoter. PCR were performed in parallel on the proximal human APC promoter corresponding to the sequence which conferred the regulation by RIP140 in the luciferase assays, on an upstream region (control) and on the CCNE2 promoter (both used as negative controls). As shown in Figure 6D, we found significant amplifications of all three regions after anti-histone H3 ChIP. By contrast, a specific recruitment of RIP140 (as compared to the use of an irrelevant antibody only) was detected on the APC promoter thus identifying the *APC* gene as a direct transcriptional target of RIP140.

In order to demonstrate that the regulation of APC was indeed required for the regulation of β-activation by RIP140, we used HCT116 cells with APC overexpression or depletion which was assessed by quantification of the APC mRNA levels (Figure 6E) which led to a regulation of ABC staining mainly after ectopic expression of APC (Figure 6F). Very interestingly, the inhibition of ABC staining by RIP140 was lost when APC expression was modulated (Figure 6G) indicating that RIP140 activity was dependent of APC gene regulation.

To further support the role of APC in RIP140 activity in colon cancer cells, we used SW480 cells which expressed a mutated form of APC (29) and stably engineered these cells to overexpress GFP-RIP140 (SW-RIP cells) or GFP alone (SW-GFP cells) (Supplementary Figure 5A). The effect of RIP140 overexpression on in vitro cell proliferation (Supplementary Figure 5B) and on tumor growth after xenografting (Supplementary Figure 5C) was significantly less intense in stably transfected SW480 cells as compared to HCT116 cells (Figure 4B and C). The effect of RIP140 on β-catenin activation was also milder in SW480 cells as compared to HCT116 cells (Supplementary Figure 5D).

Decreased expression of the *RIP140* gene in human colon cancers

To determine the biological relevance of our results in human pathology, we first quantified *RIP140* gene expression in human colon cancer samples as compared to normal colon tissues. We first reanalyzed the published Affymetrix DNA microarray data for 17 normal tissues and 22 colon cancers (30). As shown in Figure 7A, results clearly showed a significant decrease of RIP140 mRNA levels in colon cancer biopsies. We confirmed these findings by RT-qPCR analysis of 24 pairs of normal

and tumor colon tissue samples showing a decrease of RIP140 expression in almost 60% of the tumors (Figure 7B).

In order to emphasize the decreased expression of the *RIP140* gene in colon cancer, we performed an immunohistochemical analysis using an anti-RIP140 antibody on a tissue microarray (TMA) containing 24 adenocarcinoma samples matched with the corresponding normal tissues. As observed at the mRNA level, we noticed a significant decrease of nuclear RIP140 positive cells in 60% of the colon adenocarcinoma as compared to the normal tissues (Figure 7C).

We also searched for a correlation between *RIP140* and *APC* gene expression in human colon biopsies. In perfect agreement with the data from mice and human colon cancer cell lines, the reanalysis of a transcriptomic study performed in a cohort of 396 colon cancers (31) revealed a very significant positive correlation between the expression of the two genes at the mRNA level (Figure 7D). We also assessed the correlation between APC and RIP140 expression in a subset of tumors with microsatellite instability which exhibit fewer losses or gains of chromosomal regions (32). In these tumors, the direct regulation of *APC* gene transcription by RIP140 should lead to a stronger correlation of their mRNA levels since no LOH in chromosome 5q would affect *APC* gene expression. As shown in Supplementary Figure 6, we found that the correlation between *APC* and *RIP140* expression was indeed stronger in microsatellite-unstable (rho= 0.659) than in microsatellite-stable (rho= 0.439) tumors. Finally and as expected, RIP140 expression was inversely correlated with β-catenin target genes such as *c-Myc* (MYC) or *Gastrin* (GAST) in the whole cohort (Figure 7D). Altogether, these data clearly demonstrated that colon tumorigenesis is associated with a decrease in RIP140 expression both at the mRNA

and protein levels which is inversely correlated with the activation of the Wnt signaling.

RIP140 expression as a prognostic marker in colon cancer

The results obtained in colon cancer cells and in patients led us to look for a link between RIP140 expression and colon cancer prognosis. As a first approach to demonstrate that low RIP140 expression in colon cancer could be associated with a shorter survival, we used the *RIPKO* mouse model bred with the tumor-prone $Apc^{\Delta 14/+}$ mouse strain (5). These mice bear a germline invalidation of the *Apc* gene due to deletion of exon 14 which mimics human familial adenomatous polyposis (FAP) by the severity of colon tumorigenesis. In this Apc-invalidated background, the loss of one *Rip140* allele strongly affected the lifespan of these mice. As shown in Figure 8A, Kaplan-Meier plots revealed that mice heterozygous for both the *Apc* and *Rip140* genes died earlier than $Apc^{\Delta 14/+}$ mice bearing the wild-type *Rip140* gene. These mouse experiments thus strongly supported the hypothesis that RIP140 expression could be associated with survival in colon cancer patients.

In support of this hypothesis, using the same set of tumors as in Figure 7A, we found that patients with high RIP140 mRNA levels in the tumor presented better rates of overall survival than patients with low RIP140 mRNA levels (Figure 8B). RIP140 expression was also found significantly correlated with progression free survival in two independent cohorts (Supplementary Figure 7A and B). Moreover, as shown in Figure 8C, data obtained from labeling of a TMA containing 59 adenocarcinoma samples indicated that overall survival rates were higher in patients bearing tumors with a high RIP140 expression than those with tumors expressing low levels of

RIP140. Altogether, these results demonstrate that RIP140 expression decreases during colon tumorigenesis and is associated with poor patient survival.

DISCUSSION

In the present study, we demonstrate that the transcriptional repressor RIP140 is involved in the regulation of intestinal epithelium homeostasis and tumorigenesis. Based on in vivo experiments using transgenic mice, our study first identified RIP140 as a new regulator of intestinal epithelium homeostasis through its significant impact on cell proliferation and apoptosis. Indeed, using both gain and loss-of-function approaches, our data reveal that RIP140 strongly inhibits cell proliferation and programmed cell death in the intestinal epithelium. Our data also demonstrated that RIP140 plays an important role in colon cancer cells inhibiting cell cycle progression and cell proliferation in vitro and in vivo after grafting onto nude mice.

Our work clearly demonstrates that RIP140 acts as a new inhibitor of the Wnt signaling pathway through the regulation of β-catenin activation (see Figure 8D). Indeed, RIP140 overexpression clearly inhibited the levels of active β-catenin both in transgenic mice, in human colon cancer cells and biopsies. This effect was observed by measuring the level of unphosphorylated active β-catenin, by quantifying the expression of several β-catenin target genes and by analyzing the regulation of a transiently transfected β-catenin responsive reporter construct. Such a regulation of the Wnt/APC/β-catenin signaling by RIP140 could explain its effect on intestinal homeostasis and tumorigenesis since many studies have demonstrated the importance of the Wnt pathway in controlling these processes. For instance, the loss of APC function or altered β-catenin/TCF4 signaling in intestinal epithelium led to enhanced proliferation and apoptosis (33).

However, other nuclear signaling pathways targeted by RIP140 such as nuclear receptors (7) and E2Fs (8) could mediate some of the effects that we observed. Indeed, several NRs exhibit a strongly deregulated expression in intestinal epithelium

and have been shown to play an important physiopathological role in the intestine (34). For instance, receptors such as LRH-1 have pro-mitotic activity while others such as VDR, ERβ and FXR play an anti-tumor role in mice (35). Some of these effects are mediated by regulating the Wnt/APC/β-catenin signaling by the corresponding NRs (36). By contrast, few data are available on the role of E2Fs in the intestine although a recent study revealed that E2F4 determines cell cycle progression in normal intestinal epithelial crypt cells (37) while another study reported the role of Rb in the maintenance of enterocyte quiescence (38).

Interestingly, our work demonstrated that RIP140 directly induces the transcription of the tumor suppressor *APC* gene. Indeed, RIP140 is recruited on the *APC* gene promoter and increased its transcription in transient transfection experiments. More importantly, RIP140 and APC expression were significantly correlated in mouse intestinal epithelium, in human colon cancer cell lines and in human tumor biopsies. Although very few studies on the *APC* gene promoter have been published, several functional binding sites have been found in the human promoter sequence (26) and further work will be necessary to decipher the precise underlying molecular mechanisms.

Our data clearly indicate that the effects of RIP140 on β-catenin activation rely on the regulation of APC expression in human colon cancer cells. This observation could also be relevant in colon cancer cells bearing a mutation in the *APC* gene (see data on SW480 cells in Supplementary Figure 5), in line with a recent study demonstrating that truncated APC controls proliferation and β-catenin activity in colorectal cancer cell lines (39). However, more complex mechanisms could be implicated in physiological conditions. Indeed, in the mouse intestinal epithelium, RIP140 regulates the expression of other members of the β-catenin destruction complex such as the

Csk1E and *Axin2* genes. The positive regulation of the *Axin2* gene was surprising since one would have expected an inhibition by RIP140 as for other β-catenin target genes. This suggests that other transcription factors which control the expression of the *Axin2* gene might be positively regulated by RIP140. Interestingly, the Axin2 promoter encompasses a CG rich region with Sp1 binding sites which might support such a transcriptional increase in response to RIP140 as we previously reported for several promoters containing Sp1 binding sites (28).

Our results also demonstrate that RIP140 expression is finely regulated in both the normal and tumoral intestinal epithelia. The *RIP140* gene is expressed in epithelial cells, with a stronger expression in differentiated cells of villus than in proliferating cells of the crypt. The same gradient of *APC* gene expression was observed along the crypt-villus axis, where it counteracts β-catenin signaling and allows differentiation (40). We also showed that RIP140 expression (both at the mRNA and protein levels) strongly decreased during tumorigenesis. An attractive hypothesis to explain all these regulations is that RIP140 expression is negatively controlled by the Wnt/APC/β-catenin pathway itself. Several negative transcriptional responses to activation of the Wnt/APC/β-catenin pathway have been reported (41) and a negative transcriptional element (sequence AGAWAW) has been identified in the promoter of the repressed genes (42). A bioinformatics analysis of the *RIP140* gene promoter identified two AGAWAW sites in the proximal region. The existence of such a transcriptional regulatory loop would explain the low expression of the *RIP140* gene in proliferating crypts and in colon tumors which exhibit constitutively high Wnt/APC/β-catenin activity and might indicate that RIP140 expression must be tightly controlled to avoid deleterious effects on cells.

Lastly, our work demonstrated that patients whose tumors contained high levels of RIP140 had better progression free and overall survival rates than patients whose tumors had low levels of RIP140. Further studies are now required to define the clinical relevance of RIP140 as a prognostic marker as compared to the previously reported gene signatures (43). These data, linking *RIP140* gene expression with patient survival, were supported by the decreased lifespan of mice bearing the $Apc^{\Delta 14/+}$ deletion associated with the loss of one allele of the *Rip140* gene. It should be noted that during the crossing experiments, we did not obtain *Rip140* null animals in the $Apc^{\Delta 14/+}$ background suggesting that such double transgenic animals are not viable. Altogether, our results strongly suggest that RIP140 acts as a modifier gene of the APC mutated phenotype in colon tumorigenesis. Indeed, it is now well known that although the *APC* gene is considered as the central gatekeeper gene in colon cancer, several genetic modifiers (such as the Mom genes for *Modifier of Min 1*) have been identified and connect myriad factors that determine the course of the disease (for a review see (4)). *In vivo* experiments using chemical-induced carcinogenesis would also confirm the relevance of RIP140 in the initiation of colon tumorigenesis. A first experiment using azoxymethane and dextran sulfate sodium in RIPKO mice led to a stronger inflammatory response associated with histological abnormalities as compared to wild-type littermates (data not shown). In line with all these observations, a recent study performed in colon cancer samples by the Cancer Genome Atlas Network reported a mutation in the RIP140 gene which encoded a truncated protein together with several non-synonymous SNPs introducing amino-acid changes in the RIP140 coding sequence (44). Interestingly, another frame shift mutation was previously reported in patients with familial colon cancers (45).

In summary, this study uncovers the role of RIP140 in intestinal homeostasis and colorectal carcinogenesis. In addition, these results identify RIP140 as a new regulator of *APC* gene transcription and as an inhibitor of the Wnt/APC/β-catenin pathway. Although several molecular events involved in tumor progression have been identified, the full sequence of steps leading to cancer is still to be established. Our findings extend the knowledge of the role and mechanism of action of the *RIP140* gene at a molecular level and highlight, at a clinical level, the potential value of RIP140 as a biomarker with diagnostic, prognostic or therapeutic interest in colon cancer.

METHODS

Animals. C57BL/6J *Rip140* -/- (*RIPKO*) mice (12) were given by Pr MG Parker (Imperial College London, London, UK). C57BL/6/129 *RIP140* transgenic (*RIPTg*) mice were generated using the Speedy Mouse® Technology (Nucleis) by insertion of a single copy of the human RIP140 cDNA at the *HPRT* locus. The coding sequence of the human RIP140 gene (BclI/ClaI fragment) was cloned into the BamHI site of the Gateway® pENTR-1A vector (Invitrogen) previously modified to include the rabbit β-globin polyA sequence and the CAG promoter. The transgene was then transferred into the pDEST-HPRT vector (Nucleis) which was linearized using AgeI and electroporated into HPRT-deficient BPES-embryonic stem (ES) cells by standard methods. This construct contained two regions of homology with the HPRT gene which allowed insertion of the transgene at this locus. The ES clones with homologous recombination were selected on hypoxanthine-aminopterin-thymidine (HAT) supplemented medium and genotyping of HAT-resistant ES clones was performed by PCR analysis of genomic DNA using primers in the RIP140 gene and in the poly (A) sequence (see Table S1). Targeted ES cells were injected into C57BL/6-derived blastocysts that were then transplanted into the uteri of recipient females. Resulting chimeric males were bred with C57BL/6 females, and the F1 agouti female off-springs were backcrossed with C57BL/6 males. Animals were genotyped by qPCR using RIP140 primers. The tumor-prone *Apc*$^{\Delta 14/+}$ mouse strain was obtained from Dr C Perret (Institut Cochin, Paris) (5). These mice bear a germline invalidation of the *Apc* gene due to deletion of exon 14 and develop intestinal lesions mainly in the colon. All animals were maintained under standard conditions, on a 12:12-h light/dark schedule and fed a chow diet *ad libitum*, according to European Union guidelines for use of laboratory animals. *In vivo* experiments were

performed on male and female mice in compliance with the French guidelines for experimental animal studies (agreement B34-172-27).

Whole body irradiation. Mice (12 week-old) were anesthetized (*i.p.* injection of ketamine and xylazine), placed into a ventilated Plexiglas pie container and underwent 12 Gy whole-body irradiation (WBI) using a Shephard 137Cs-ray irradiator at a dose rate of 4.21Gy/min, following biosafety guidelines of the Val d'Aurelle hospital. Mice were killed 2.5 days after WBI and small intestine was removed for histological analyses. Number and length of regenerating villi together with length of survival crypts were quantified (24 fields per genotype using x10 magnification) in small intestine after hematoxylin-eosin staining of paraffin sections (9 animals per group).

EdU detection in mouse tissues. Mice were injected *i.p.* with 100-200µg of 5-ethynyl-2'-deoxyuridine (EdU, Invitrogen) in PBS. Small intestine was removed 2h after injection, paraformaldehyde-fixed, embedded in paraffin and sectioned. After paraffin removal, sections were permeabilized with 0.5% Triton X100-PBS during 30 min at room temperature and then washed with 3% BSA-PBS. EdU incorporation was detected using the Click-iT® EdU cell proliferation kit as recommended by the manufacturer (Invitrogen). Following two rinses with PBS, slides were counterstained with Hoechst and mounted for fluorescence microscopy.

Real-time quantitative PCR (RT-qPCR). Total RNA was extracted from cells or mouse tissues using High Pure RNA Isolation kit (Roche Applied Science) according to the manufacturer's instructions. Sequential isolation of wild-type mouse small intestinal epithelial cells was performed as described (46). Total RNA (1µg) was subjected to reverse-transcription using Superscript II reverse transcriptase (Invitrogen). RT-qPCR were performed with the LightCycler® 480 SYBR Green I

Master (Roche Applied Science) and were carried out in a final volume of 10µl using 0.25µl of each primer (25µM), 5µl of the supplied enzyme mix, 2.5µl of H2O and 2µl of the template diluted at 1:10. After pre-incubation at 95°C, runs corresponded to 35 cycles of 15s each at 95°C, 5s at 60°C and 15s at 72°C. Melting curves of the PCR products were analyzed using the LightCycler® software to exclude amplification of unspecific products. Results were normalized to RS9 or 28S housekeeping gene transcripts. See Supplemental Table S1 for primer sequences.

ChIP analysis. For ChIP analysis, HCT116 cells (70% confluent) were cross-linked with 3,7% formaldehyde during 10 min at 37°C. The Champion ChIP One-Day Kit (Qiagen) was then used according to the manufacturer's recommendations. Immunoprecipitations were performed using rabbit polyclonal antibodies against acylated-H3 (06-599, Upstate), RIP140 (Ab42126, Abcam) or an irrelevant IgG antibody as a control. Quantitative PCR was then performed using a LightCycler® 480 SYBR Green I Master (Roche Applied Science) with 2µl of material per point. Primers flanking the RIP140 site of the APC promoter are given in Supplemental Table S1. The input DNA fraction corresponded to 5% of the amount of immunoprecipitated chromatin.

Histological and immunufluorescence analysis. Mouse tissues were fixed with 4% paraformaldehyde, embedded in paraffin and sectioned (5µm). Histological analyses were realized by hematoxylin-eosin coloration of paraffin-embedded tissue sections. For immunufluorescence analyses, following incubation in citrate buffer solution, paraffin-embedded tissue sections were incubated with blocking serum for 3h to reduce non-specific binding. Sections were then incubated with antibodies specific for RIP140 (Ab42126, Abcam), active β-catenin (05-665, clone 8E7, Millipore) and total β-catenin (610153, clone 14, BD Transduction Laboratories). IF

revelation was performed using an Alexa-conjugated secondary antibody (Invitrogen). After washing, sections were counterstained with Hoechst (Sigma Aldrich) and mounted for fluorescence microscopy. Negative controls using rabbit or mouse IgGs were performed and no staining was observed in these conditions. The staining quantification was performed at either x20 or x40 magnifications (24 fields per genotype corresponding to 6 different animals) by determining the mean of fluorescence intensity and staining area, using the measurement and colocalization module available on AxioVision v4.7.1 software (Carl Zeiss).

Cell culture and transfections. HCT116 human colon adenocarcinoma cells were stably transfected with the empty pEGFP vector (Clontech) or with the same vector containing the full-length human RIP140 cDNA (25). Pools of G418 resistant cells (respectively named HCT-GFP and HCT-RIP) were selected and grown in McCoy medium supplemented with 10% FCS, 100U/ml penicillin, 100mg/ml streptomycin, 100mg/ml sodium pyruvate and 750µg/ml G418. To determine the fraction of cells in G1 and S phases, HCT116 cells were transiently transfected with cdt1-RFP Premo™ Fucci Cell Cycle Sensor (Invitrogen) and incubated with EdU (then detected as described above for mouse tissues). After fixation and mounting, Fucci and Edu fluorescent signals were quantified only in GFP and GFP-RIP140 positive cells in order to determine the percentage of cells in G1 phase (Fucci positive) and in S phase (EdU positive). All transfections were carried out using Lipofectamine2000 (Invitrogen) as recommended by the manufacturer.

Luciferase assays. Stably transfected HCT116 cells and mouse embryonic fibroblasts (MEF) derived from wild-type or RIPKO mice (12) were transfected with the pTOPflash or pFOPflash reporter vectors and treated or not with a Wnt3a conditioned medium (47). HCT116 cells were tranfected with a *APC* gene promoter

reporter vector or the same reporter plasmid bearing the SV40 promoter together with a plasmid allowing RIP140 expression (pEF-c-mycRIP140 (48)). Cells were plated in 96-well plates (3.10^4 cells per well) 24h prior to DNA transfection with Jet-PEI (200ng of total DNA). The pRLCMVBis plasmid (Ozyme) was used to normalize transfection efficiency. Firefly luciferase values were measured and normalized by the Renilla luciferase activity. For the TOP/FOP assay, values were expressed as the mean ratio of pTOPflash/pFOPflash luciferase activities.

Immunoblotting. After transfection, nuclear and cytoplasmic protein extracts were prepared using the NE-PER kit (Thermo Scientific) and cell extracts were analyzed by Western blotting using a primary antibody against RIP140 (Ab42125; Abcam), β-catenin (active or total) or β-actin (A2066, Sigma Aldrich). Signals were revealed using a horseradish peroxidase-conjugated secondary antibody (Jackson ImmunoResearch) and enhanced chemiluminescence (ECL-Plus; GE Healthcare) according to the manufacturer's instructions.

Tumorigenicity assay. 6 week-old nu/nu female mice from Harlan Laboratories, housed in a pathogen-free facility, were used to assess the effect of RIP140 on tumor growth. HCT-GFP and HCT-RIP cells (8.10^5 cells) were injected subcutaneously and tumor formation was monitored every 3 days using a caliper. Tumor volume was calculated as width x length x thickness. Mice were sacrificed 40 days after injection.

Cell proliferation assay. Stably transfected HCT116 cells (HCT-GFP and HCT RIP cells) were seeded at a density of 2500 cells/well into E-Plate 16 (ACEA Biosciences, Inc., San Diego, CA) containing 150µl per well of medium supplemented with 10% FCS. Dynamic monitoring of cell growth was determined every 24 hours during 4 days using the impedance-based xCELLigence system (Roche Applied Science,

Germany). The cell index was derived from measured cell-electrode impedance that correlates with the number of viable cells.

DNA microarray analysis. Published DNA microarray data (30) (31) were reanalyzed for *RIP140*, *APC*, *MYC* and *GAST* expression. The optimal threshold values, which induced the best discrimination according to the disease progression status, were calculated to maximize the Youden's index. This index is defined as the sum of sensitivity and specificity minus 1 and is frequently used to dichotomize continuous variable in Receiver Operating Characteristic (ROC) curve methodology.

Tissue microarrays. Tissue microarrays (TMA) contained samples from 24 matched paraffin blocks from identified patients with primary colon cancer and adjacent normal tissue (T8235790d, Biochain) or from 59 patients with adenocarcinoma (CD4, SuperBiochip). Three-micrometer sections of the TMA were deparaffinized and rehydrated in graded alcohols. Following epitope retrieval treatment in citrate buffer and neutralization of endogenous peroxidase, TMA sections were incubated overnight at 4°C with the anti-RIP140 (Ab42126, Abcam). Immunohistochemical labeling was revealed using peroxydase-conjugated anti-rabbit secondary antibodies (Jackson Immunoresearch) and 3,3'-Diaminobenzidine (DAKO cytomation) as a substrate. Sections were counterstained with hematoxylin. Images were taken using NanoZoomer (Hamamatsu Photonics) and the percentage of stained nuclei was quantified using TissueQuest software (TissueGnostic).

Statistical analysis. Data were presented as means ± S.D. Statistical comparisons were performed with Mann-Whitney or Spearman tests. Differences were considered statistically significant at $p<0.05$. Progression Free Survival (PFS) was calculated from the start of palliative chemotherapy until disease progression or last follow-up. Patients who died without progression were censored at the time of death. Overall

Survival (OS) was calculated from the start of palliative chemotherapy until death. Patients lost to follow-up were censored at the time of last contact. The Kaplan-Meier method was used to estimate PFS and OS. The log-rank test was used to test the differences between groups which were considered statistically significant at the $p<0.05$ level. STATA statistical software (STATA, College Station, TX) was used for all analyses.

ACKNOWLEDGMENTS

We thank the Réseau d'Histologie Expérimentale de Montpellier (RHEM) for histology facilities and Dr F. Bernex for her expertise. We are grateful to Dr. J. Zilliacus (Karolinska Institutet Novum) for the kind gift of the pEGFP-C2-RIP140 vector, to Dr S. Narayan (University of Florida) for providing the APC reporter construct, to Dr P. Forgez (CdR Saint-Antoine) for the APC expression vector and to Dr A. Coquelle (INSERM U896) for the Fucci/G1 plasmid. We also thank Dr S. Fritsch for initial characterization of the *RIPTg* mice and to Drs C. Teyssier for critical reading of the manuscript. This work was supported by INSERM, Université de Montpellier 1, Fondation Lejeune, INCa (2011-054), SIRIC Montpellier and the Institut régional du Cancer de Montpellier (ICM).

REFERENCES

1. Schneikert J, Behrens J. The canonical Wnt signalling pathway and its APC partner in colon cancer development. *Gut*. 2007;56(3):417–425.

2. Klaus A, Birchmeier W. Wnt signalling and its impact on development and cancer. *Nat Rev Cancer*. 2008;8(5):387–398.

3. Zeng X et al. A dual-kinase mechanism for Wnt co-receptor phosphorylation and activation. *Nature*. 2005;438(7069):873–877.

4. Kwong LN, Dove WF. APC and its modifiers in colon cancer. *Adv Exp Med Biol*. 2009;656:85–106.

5. Colnot S et al. Colorectal cancers in a new mouse model of familial adenomatous polyposis: influence of genetic and environmental modifiers. *Lab Invest*. 2004;84(12):1619–1630.

6. Cavailles V et al. Nuclear factor RIP140 modulates transcriptional activation by the estrogen receptor. *EMBO J*. 1995;14(15):3741–3751.

7. Augereau P et al. The nuclear receptor transcriptional coregulator RIP140. *Nucl Recept Signal*. 2006;4:e024.

8. Docquier A et al. The transcriptional coregulator RIP140 represses E2F1 activity and discriminates breast cancer subtypes. *Clin Cancer Res*. 2010;16(11):2959–2970.

9. Christian M, Tullet JM, Parker MG. Characterization of four autonomous repression domains in the corepressor receptor interacting protein 140. *JBiolChem*. 2004;279(15):15645–15651.

10. Yang X-J, Seto E. Lysine acetylation: codified crosstalk with other posttranslational modifications. *Mol Cell*. 2008;31(4):449–461.

11. Docquier A et al. The RIP140 Gene Is a Transcriptional Target of E2F1. *PLoS ONE*. 2012;7(5):e35839.

12. White R et al. The nuclear receptor co-repressor nrip1 (RIP140) is essential for female fertility. *NatMed*. 2000;6(12):1368–1374.

13. Leonardsson G et al. Nuclear receptor corepressor RIP140 regulates fat accumulation. *ProcNatlAcadSciUSA*. 2004;101(22):8437–8442.

14. Duclot F et al. Cognitive impairments in adult mice with constitutive inactivation of RIP140 gene expression. *Genes Brain Behav*. 2012;11(1):69–78.

15. Nautiyal J et al. The transcriptional co-factor RIP140 regulates mammary gland development by promoting the generation of key mitogenic signals. *Development*. 2013;140(5):1079–1089.

16. Fritah A, Christian M, Parker MG. The metabolic coregulator RIP140: an update. *Am J Physiol Endocrinol Metab*. 2010;299(3):E335–340.

17. Van der Flier LG, Clevers H. Stem cells, self-renewal, and differentiation in the intestinal epithelium. *Annu Rev Physiol*. 2009;71:241–260.

18. MacDonald BT, Tamai K, He X. Wnt/beta-catenin signaling: components, mechanisms, and diseases. *Dev Cell*. 2009;17(1):9–26.

19. Tan CW et al. Wnt signalling pathway parameters for mammalian cells. *PLoS ONE*. 2012;7(2):e31882.

20. Hlubek F et al. Heterogeneous expression of Wnt/beta-catenin target genes within colorectal cancer. *Int J Cancer*. 2007;121(9):1941–1948.

21. Kim TH, Xiong H, Zhang Z, Ren B. beta-Catenin activates the growth factor endothelin-1 in colon cancer cells. *Oncogene*. 2005;24(4):597–604.

22. Rodilla V et al. Jagged1 is the pathological link between Wnt and Notch pathways in colorectal cancer. *Proc Natl Acad Sci USA*. 2009;106(15):6315–6320.

23. Mann B et al. Target genes of beta-catenin-T cell-factor/lymphoid-enhancer-factor signaling in human colorectal carcinomas. *Proc Natl Acad Sci USA*. 1999;96(4):1603–1608.

24. Van Es JH et al. Wnt signalling induces maturation of Paneth cells in intestinal crypts. *Nat Cell Biol*. 2005;7(4):381–386.

25. Zilliacus J et al. Regulation of glucocorticoid receptor activity by 14--3-3-dependent intracellular relocalization of the corepressor RIP140. *MolEndocrinol*. 2001;15(4):501–511.

26. Jaiswal AS, Balusu R, Narayan S. 7,12-Dimethylbenzanthracene-dependent transcriptional regulation of adenomatous polyposis coli (APC) gene expression in normal breast epithelial cells is mediated by GC-box binding protein Sp3. *Carcinogenesis*. 2006;27(2):252–261.

27. Jaiswal AS, Narayan S. Upstream stimulating factor-1 (USF1) and USF2 bind to and activate the promoter of the adenomatous polyposis coli (APC) tumor suppressor gene. *J Cell Biochem*. 2001;81(2):262–277.

28. Castet A et al. Receptor-interacting protein 140 differentially regulates estrogen receptor-related receptor transactivation depending on target genes. *Mol Endocrinol*. 2006;20(5):1035–1047.

29. Nishisho I et al. Mutations of chromosome 5q21 genes in FAP and colorectal cancer patients. *Science*. 1991;253(5020):665–669.

30. Del Rio M et al. Gene expression signature in advanced colorectal cancer patients select drugs and response for the use of leucovorin, fluorouracil, and irinotecan. *J Clin Oncol*. 2007;25(7):773–780.

31. Salazar R et al. Gene expression signature to improve prognosis prediction of stage II and III colorectal cancer. *J Clin Oncol*. 2011;29(1):17–24.

32. Jass JR. Classification of colorectal cancer based on correlation of clinical, morphological and molecular features. *Histopathology*. 2007;50(1):113–130.

33. Sansom OJ et al. Loss of Apc in vivo immediately perturbs Wnt signaling, differentiation, and migration. *Genes Dev*. 2004;18(12):1385–1390.

34. Modica S et al. The intestinal nuclear receptor signature with epithelial localization patterns and expression modulation in tumors. *Gastroenterology*. 2010;138(2):636–648, 648.e1–12.

35. D'Errico I, Moschetta A. Nuclear receptors, intestinal architecture and colon cancer: an intriguing link. *Cell Mol Life Sci*. 2008;65(10):1523–1543.

36. Mulholland DJ, Dedhar S, Coetzee GA, Nelson CC. Interaction of nuclear receptors with the Wnt/beta-catenin/Tcf signaling axis: Wnt you like to know? *Endocr Rev*. 2005;26(7):898–915.

37. Garneau H, Paquin M-C, Carrier JC, Rivard N. E2F4 expression is required for cell cycle progression of normal intestinal crypt cells and colorectal cancer cells. *J Cell Physiol*. 2009;221(2):350–358.

38. Guo J, Longshore S, Nair R, Warner BW. Retinoblastoma protein (pRb), but not p107 or p130, is required for maintenance of enterocyte quiescence and differentiation in small intestine. *J Biol Chem*. 2009;284(1):134–140.

39. Chandra SHV, Wacker I, Appelt UK, Behrens J, Schneikert J. A common role for various human truncated adenomatous polyposis coli isoforms in the control of beta-catenin activity and cell proliferation. *PLoS ONE*. 2012;7(4):e34479.

40. Andreu P et al. Crypt-restricted proliferation and commitment to the Paneth cell lineage following Apc loss in the mouse intestine. *Development*. 2005;132(6):1443–1451.

41. Hoverter NP, Waterman ML. A Wnt-fall for gene regulation: repression. *Sci Signal*. 2008;1(39):pe43.

42. Blauwkamp TA, Chang MV, Cadigan KM. Novel TCF-binding sites specify transcriptional repression by Wnt signalling. *EMBO J*. 2008;27(10):1436–1446.

43. Nannini M et al. Gene expression profiling in colorectal cancer using microarray technologies: results and perspectives. *Cancer Treat Rev*. 2009;35(3):201–209.

44. Cancer Genome Atlas Network. Comprehensive molecular characterization of human colon and rectal cancer. *Nature*. 2012;487(7407):330–337.

45. Mori Y et al. Identification of genes uniquely involved in frequent microsatellite instability colon carcinogenesis by expression profiling combined with epigenetic scanning. *Cancer Res*. 2004;64(7):2434–2438.

46. Weiser MM. Intestinal epithelial cell surface membrane glycoprotein synthesis. II. Glycosyltransferases and endogenous acceptors of the undifferentiated cell surface membrane. *J Biol Chem*. 1973;248(7):2542–2548.

47. Shibamoto S et al. Cytoskeletal reorganization by soluble Wnt-3a protein signalling. *Genes Cells*. 1998;3(10):659–670.

48. Castet A et al. Multiple domains of the Receptor-Interacting Protein 140 contribute to transcription inhibition. *Nucleic Acids Res*. 2004;32(6):1957–1966.

FIGURES

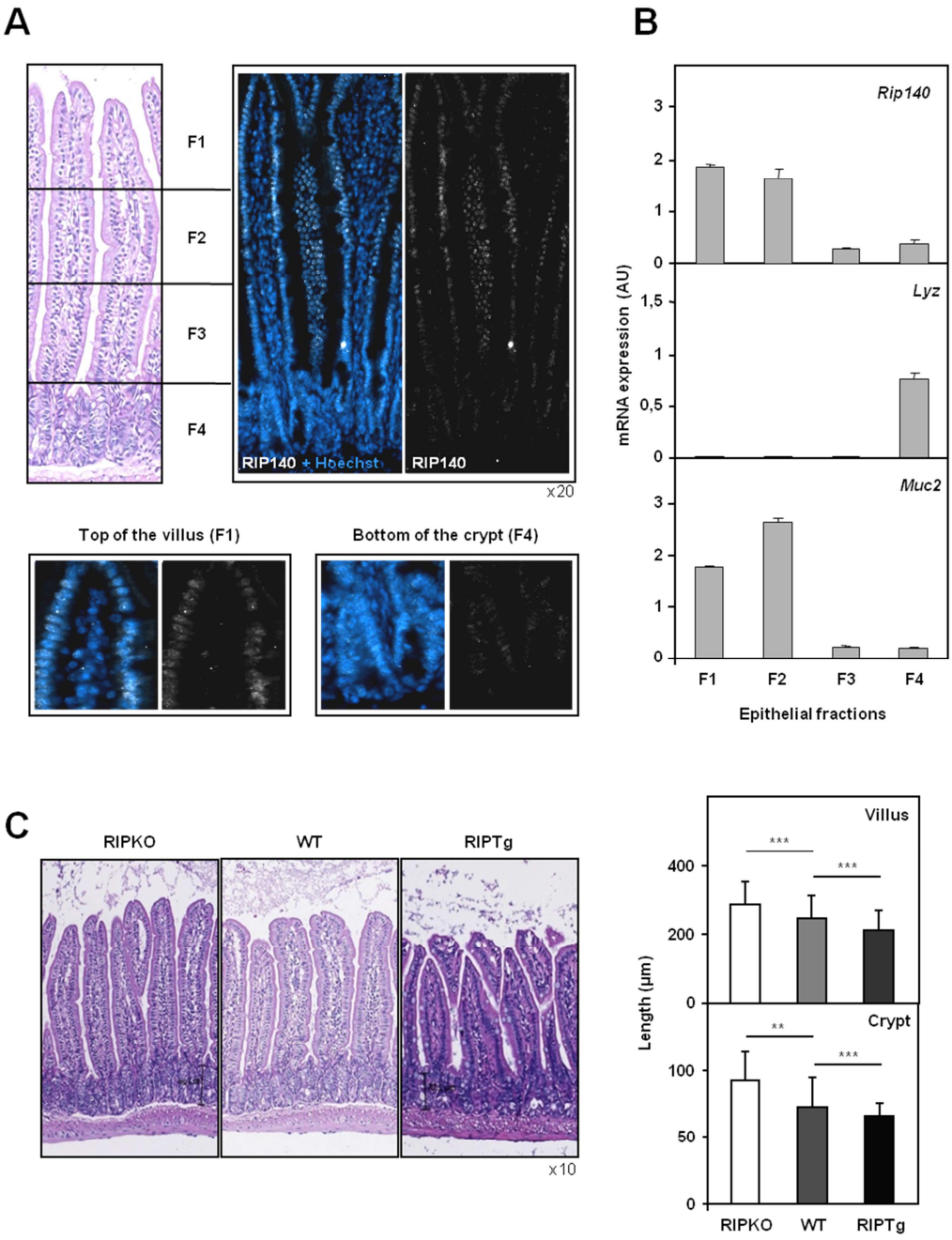

Figure 1: RIP140 expression in mouse intestinal epithelium. A) Immunofluorescence showing a gradient of RIP140 in the nuclei of epithelial cells along the villus-crypt axis of wild-type mice. **B)** RT-QPCR analysis of *Rip140* mRNA in wild-type intestinal epithelium fractions. The mRNAs encoded by the *Lyz* and *Muc2* genes were used to verify the enrichment in villus- or crypt-associated cells. Data were normalized to RS9 mRNA. The mRNA quantification for each gene are given in arbitrary units (AU) as mean ± S.D.; n=4 mice. **C)** Left panel - Hematoxylin-eosin stained transverse sections of small intestine from RIPKO, wild-type and RIPTg mice. Right panel - The length of villi and crypts was measured on at least 6 fields selected on whole intestine sections of each mouse of the three different genotypes. Values represent means ± S.D.; n=6 mice for each genotype. A Mann-Whitney U-test was used for statistical analysis (** $p<0.01$ and *** $p<0.001$).

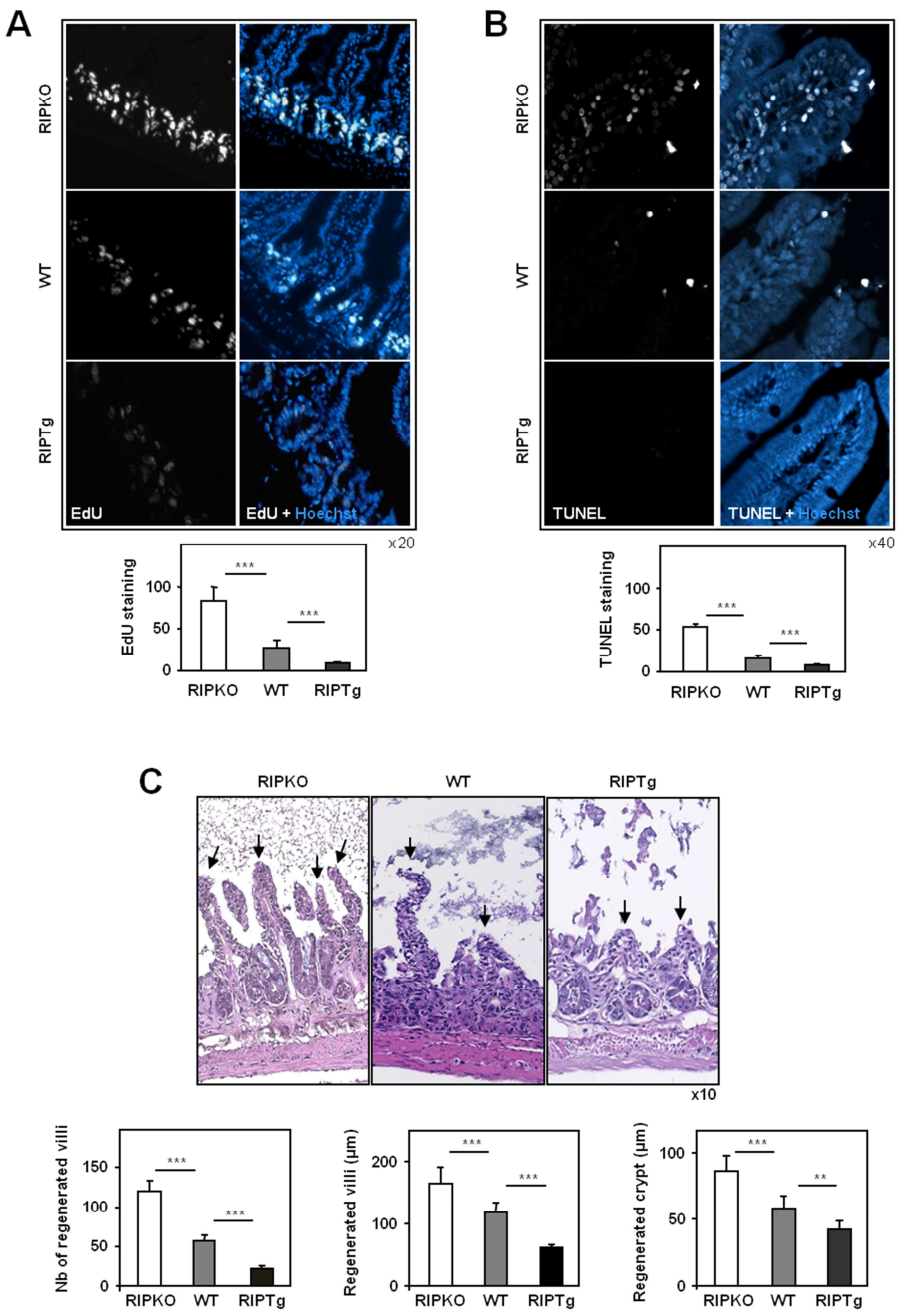

Figure 2: RIP140 inhibits intestinal cell proliferation and apoptosis. A) EdU-labeling of proliferating cells or **B)** TUNEL staining in paraffin sections of small intestine from RIPKO, wild-type and RIPTg mice. Images show merged EdU or TUNEL detection (white) and nuclear staining (blue) in small intestine. Staining are expressed as means of signal quantification ± S.D.; n=6 mice for each genotype. Original magnification ×20 for panel A and x40 for panel B. **C)** Representative hematoxylin-eosin stained transverse sections of small intestines showing crypt survival of irradiated mice (2.5 days after 12 Gy WBI). The number of surviving villi (indicated by black arrows) and the length of villi and crypts were counted in at least 6 fields of small intestine cross-sections from RIPKO, wild-type and RIPTg mice. Values are means ± S.D.; n=6 mice for each genotype, Original magnification ×10. A Mann-Whitney test was used for statistical analysis (** $p<0.01$ and *** $p<0.001$).

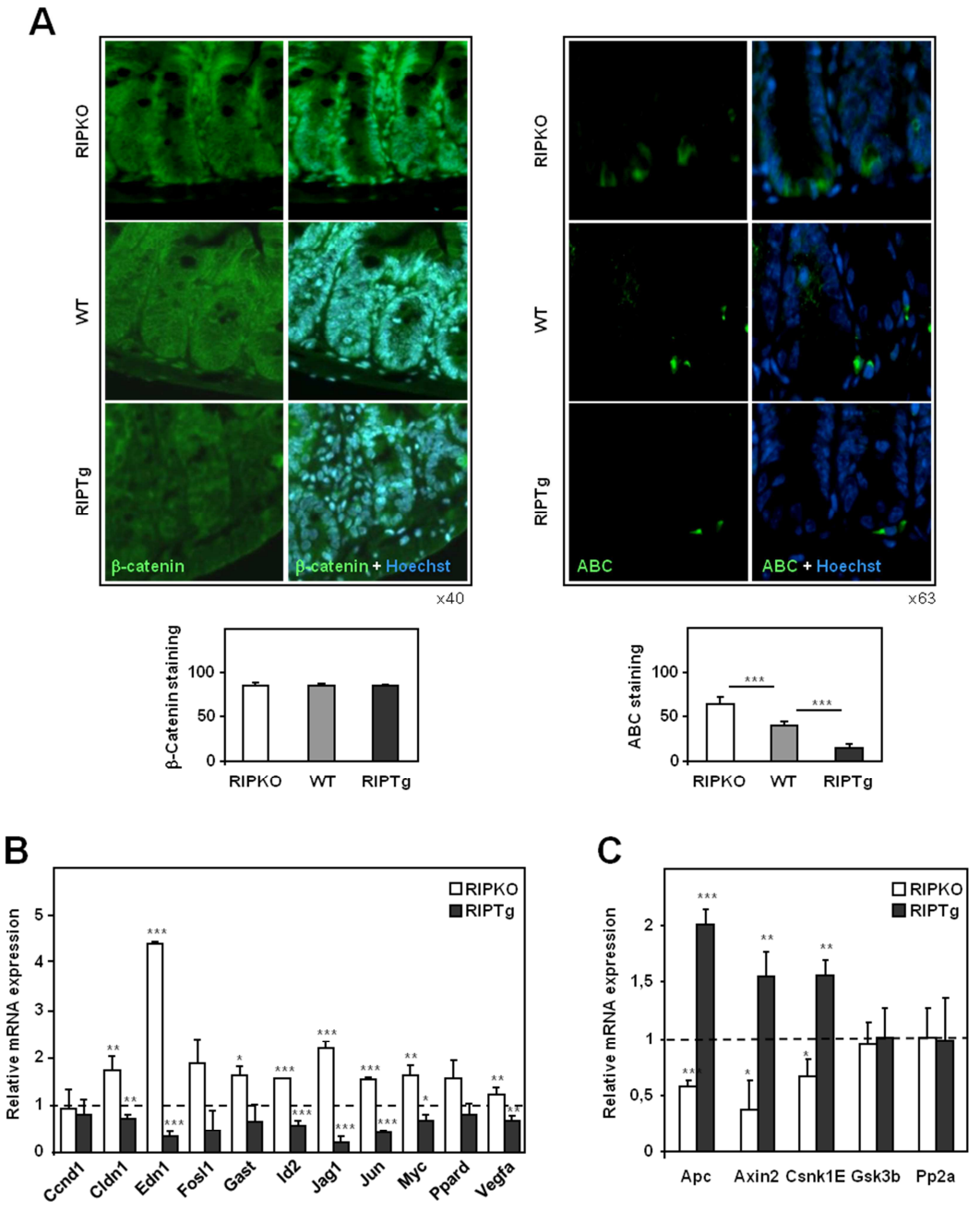

Figure 3: Activation of β-catenin by RIP140 in mouse intestinal epithelium. A) Total (left panel) and active (right panel) β-catenin in paraffin-embedded sections of small intestine from RIPKO, wild-type and RIPTg mice (β-catenin immunolabeling in green and nuclear staining in blue). Values are means ± S.D.; n=6 mice for each genotype. **B)** Expression of β-catenin regulated genes was measured by RT-qPCR analysis in RIPKO, wild-type and RIPTg mice. Values represent fold change ± S.D. *vs* levels in wild-type mice after normalization to RS9 mRNA; n=4 mice for each genotype. **C)** Same as in panel B for the expression of different members of the degradation complex. A Mann-Whitney test was used for statistical analysis (* $p<0.05$, ** $p<0.001$ and *** $p<0.001$).

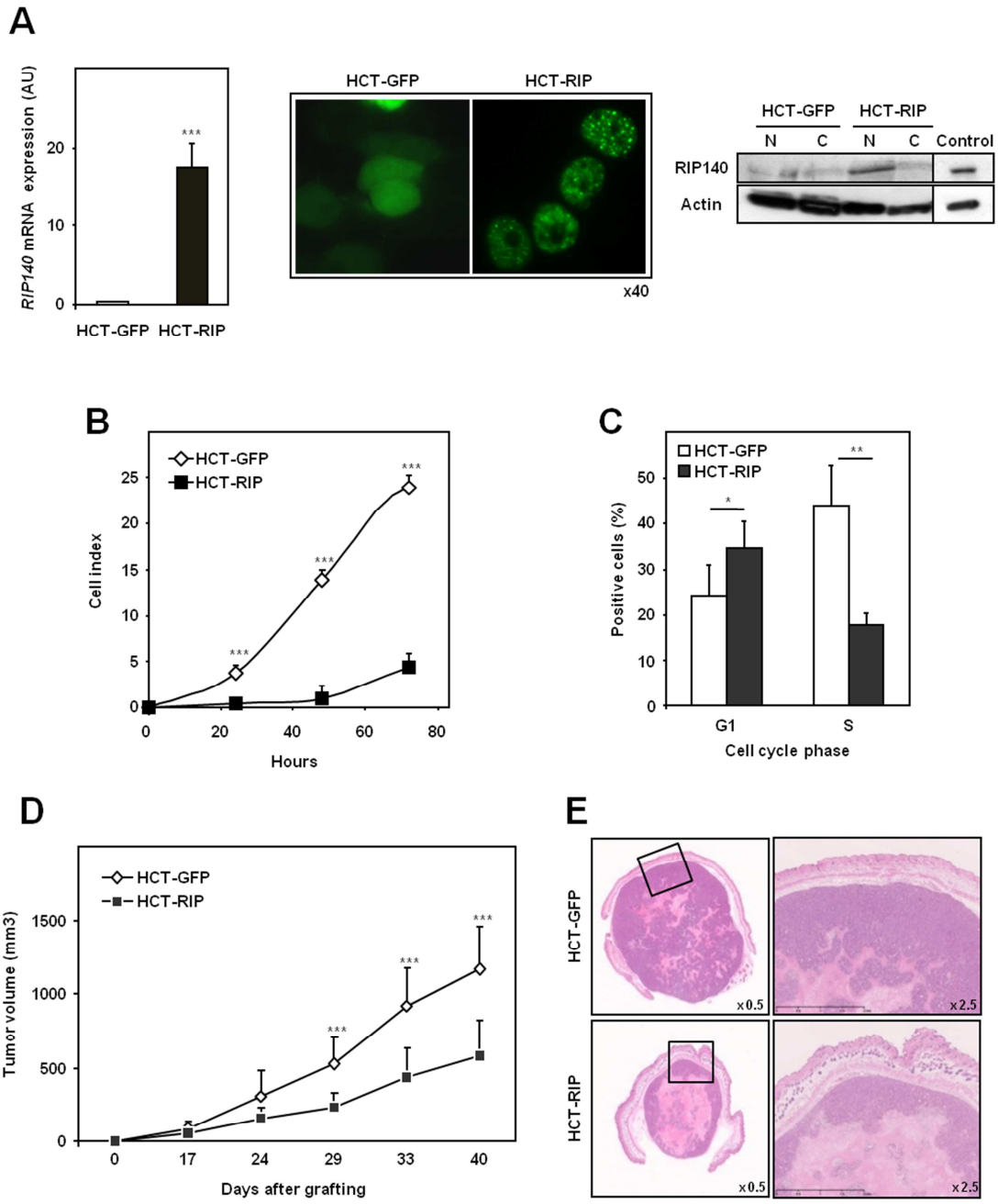

Figure 4: Effect of RIP140 on the proliferation of HCT116 human colon cancer cells. A) RT-qPCR analysis of HCT116 cells overexpressing or not RIP140. Data are expressed in arbitrary units (AU) after normalization by RS9 mRNA levels. Values are the means ± S.D.; n=5 independent experiments. The levels of RIP140 protein were detected by western-blot analysis and immunofluorescence. Blot lanes were run on the same gel but were noncontiguous. **B)** The cell index corresponding to the number of HCT-GFP or HCT-RIP viable cells was measured every 24 hours for a total duration of 72 hours. **C)** The percentages of HCT-GFP and HCT-RIP cells in G1 and S phases were determined in 10 fields. Values are means ± S.D., normalized to the total number of cells; n=5 independent experiments. **D)** The volumes of HCT-GFP and HCT-RIP cell xenografts were measured at different times after grafting. Values are means ± S.D.; n=12 xenografts per cell line. **E)** Representative necrotic areas

observed in xenograft sections stained with hematoxylin-eosin. A Mann-Whitney test was used for statistical analysis (* $p<0.05$, ** $p<0.001$ and *** $p<0.001$).

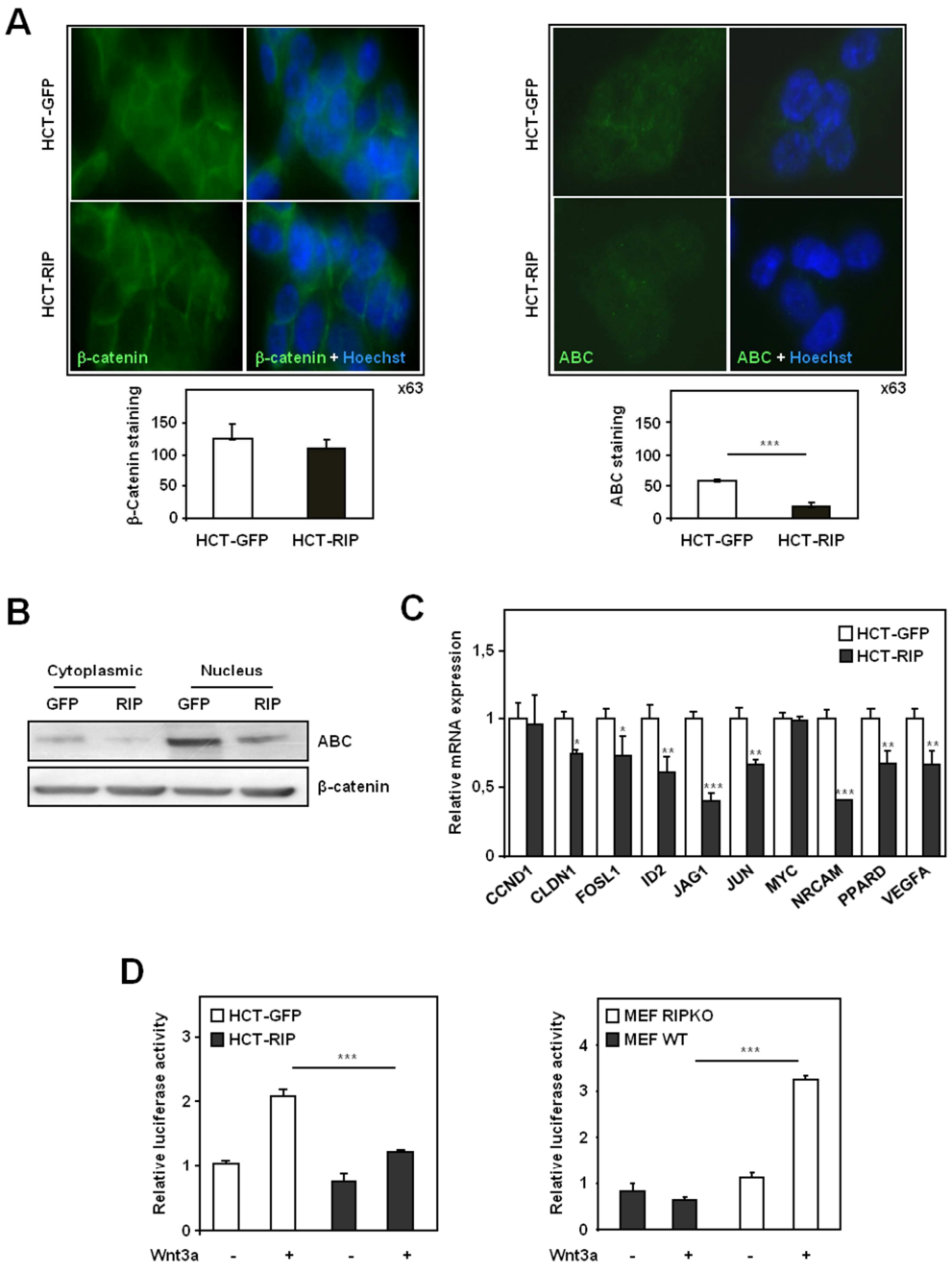

Figure 5: Regulation of β-catenin activation by RIP140 in HCT116 colon cancer cells. A) Total (left panel) and active (right panel) β-catenin in HCT-GFP and HCT-RIP colon cancer cells (β-catenin immunolabeling in green and nuclear staining in blue). Quantifications are means ± S.D. n=6 independent experiments for each cell line. **B)** The levels of total and active β-catenin (ABC) proteins were detected by western-blot analysis using specific antibodies in HCT-GFP and HCT-RIP cells. **C)** The expression of β-catenin regulated genes was measured by RT-qPCR. Values represent fold changes ± S.D. corrected by 28S mRNA and normalized to HCT-GFP cells; n=6 independent experiments for each cell line. **D)** TOP/FOP experiments were performed by transiently transfecting HCT-GFP and HCT-RIP cells (left panel) or MEF WT and MEF RIPKO cells (right panel) with the pTOPflash or pFOPflash reporter plasmids (200ng). Cells were treated or not with a Wnt3a conditioned

medium (Wnt3a). Relative luciferase activity was expressed as the mean ratio of TOP/FOP luciferase activities ± S.D.; n=3 independent experiments. A Mann-Whitney test was used for statistical analysis (* $p<0.05$, ** $p<0.001$ and *** $p<0.001$).

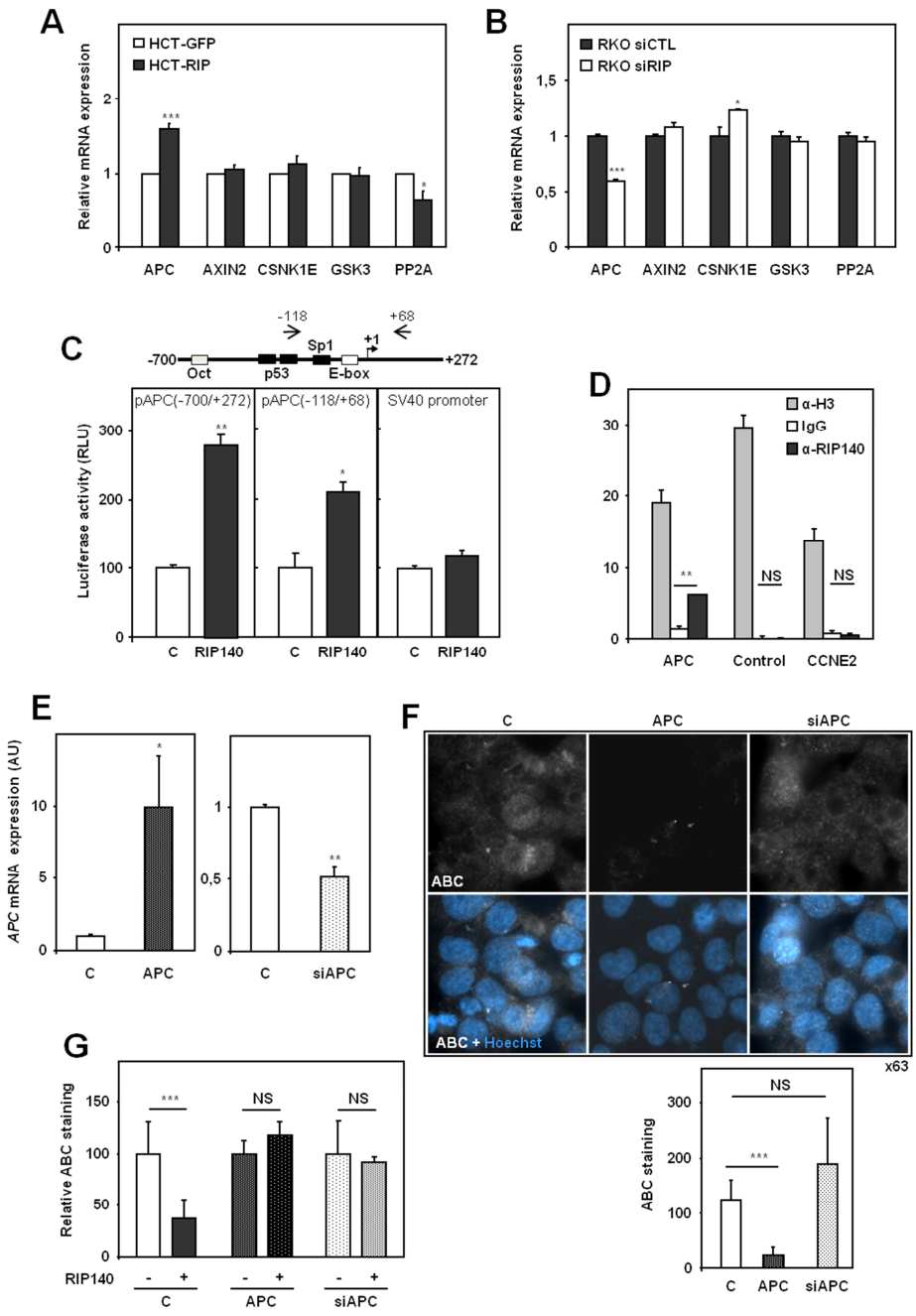

Figure 6: Regulation of *APC* gene transcription by RIP140 in human colon cancer cells. A) The expression of members of degradation complex of β-catenin was measured by RT-qPCR. Values represent fold changes ± S.D. corrected by 28S mRNA and normalized to HCT-GFP cells; n=6 independent experiments. **B)** Same as in panel A for RKO-siCTL and RKO-siRIP cells. **C)** Schematic drawing of the human *APC* gene promoter region showing experimentally characterized transcription factor binding sites. HCT116 cells were transfected with two different *APC* gene promoter reporter vectors or with an SV40 based reporter vector together or not with a RIP140 expression vector. Relative luciferase activity was expressed as means ± S.D.; n=3 independent experiments. **D)** ChIP experiments were performed on the *APC* gene proximal promoter, on an upstream region (Control) or on the CCNE2 promoter after chromatin immunoprecipitation using an antibody against total histone H3, an

antibody against RIP140 or an irrelevant antibody (IgG). **E)** The expression of APC was measured by RT-qPCR after overexpression (APC) or silencing (siAPC) of the *APC* gene. Values represent fold changes ± S.D. corrected by 28S mRNA and normalized to control cells; n=6 independent experiments. **F)** Active β-catenin immunolabeling in HCT116 cells with overexpression (APC) or silencing (siAPC) of the *APC* gene (β-catenin in green and nuclear staining in blue). Quantifications represent means ± S.D. n=3 independent experiments for each condition. **G)** Same as in panel F with overexpression or not of RIP140. In each condition, data are expressed relative to controls without overexpression of RIP140. A Mann-Whitney test was used for statistical analysis (*** $p<0.001$).

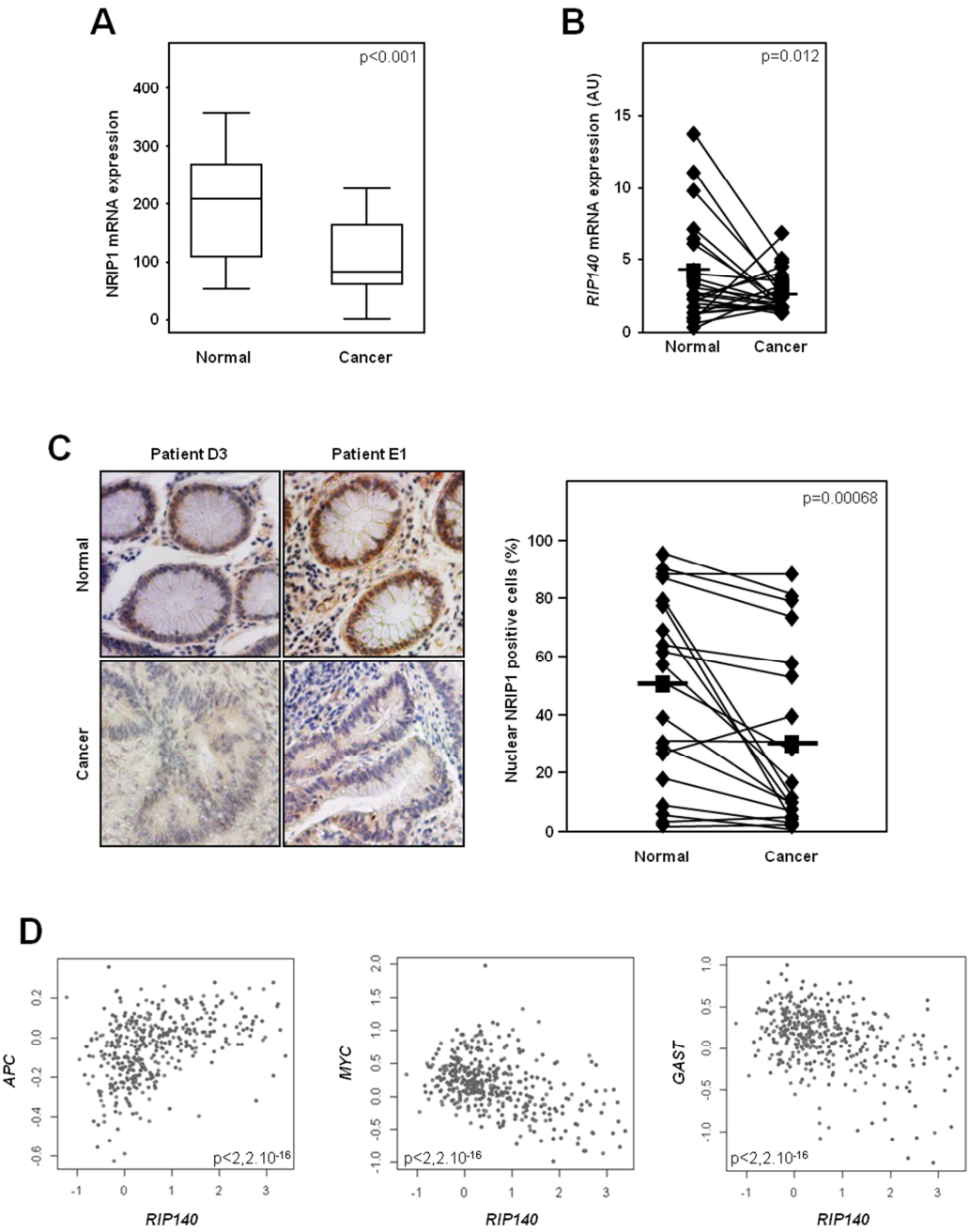

Figure 7: RIP140 expression in human colon cancers. A) RIP140 mRNA was quantified in 17 normal tissues and 22 colorectal adenocarcinomas as previously described. Data are presented as box-plots showing the median value, upper and lower quartiles and minimum and maximum non-atypical values. **B)** RIP140 mRNA levels expressed in arbitrary units (AU) after normalization to actin mRNA levels in 24 matched normal and tumor colon samples (means of the two populations are indicated as horizontal dashes). **C)** RIP140 immunochemistry of a tissue microarray containing normal mucosa of 24 patients, together with the corresponding adenocarcinoma. Nuclear RIP140-positive cells were counted and represented in a dot plot. A Mann-Whitney test was used for statistical analysis. **C)** Correlation between *RIP140* and *APC, MYC or GAST* gene expression in 396 colorectal adenocarcinomas. Statistical significance was assessed using a Spearman correlation analysis.

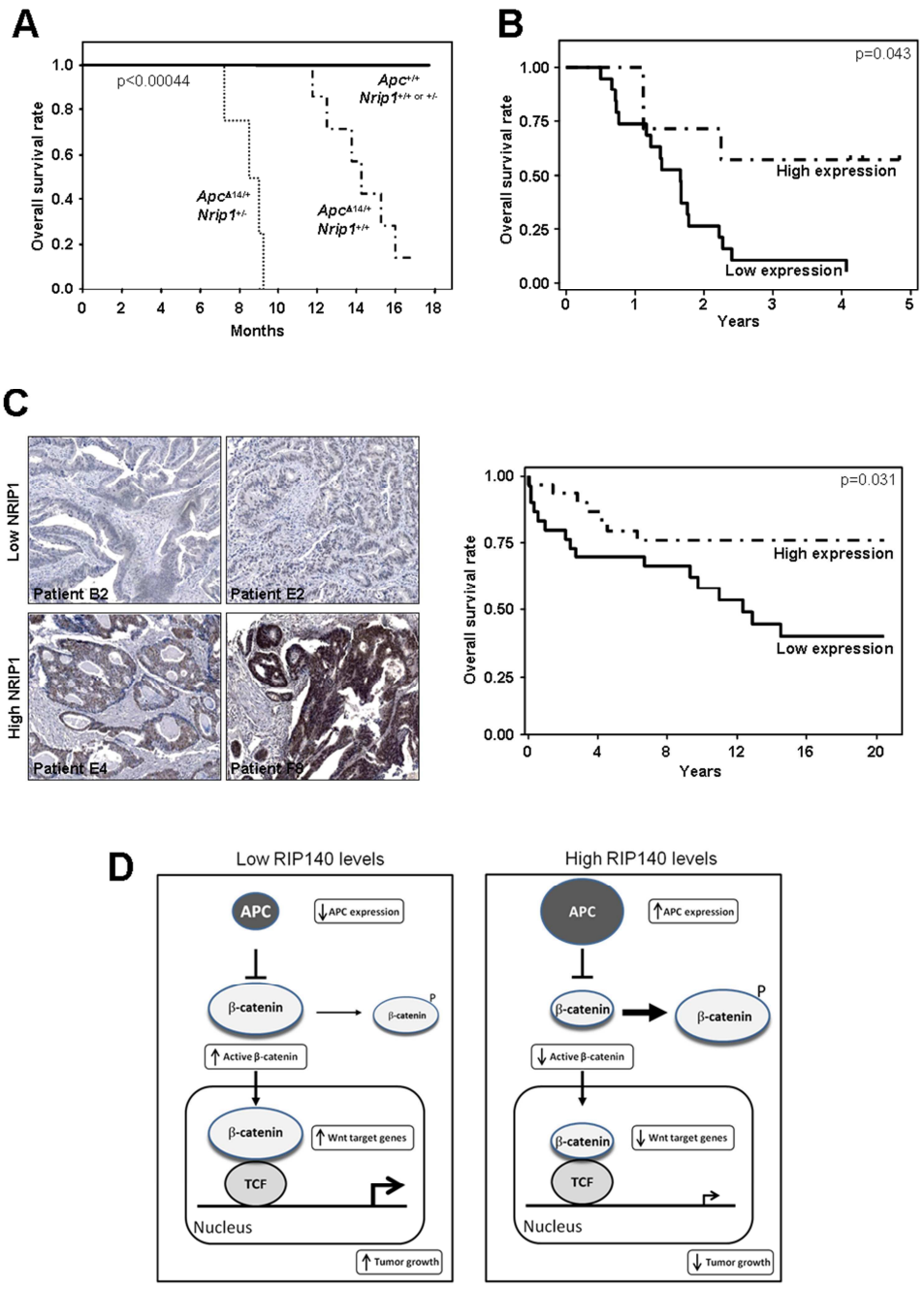

Figure 8: RIP140 is a prognosis marker in colon cancer. A) Kaplan-Meier plots of cumulative survival of *Apc*$^{+/+}$, *Apc*$^{\Delta 14/+}$ and *Apc*$^{\Delta 14/+}$/*Rip140*$^{+/-}$ mice; n= 4 mice for the *Apc*$^{\Delta 14/+}$/*Rip140*$^{+/-}$ genotype and 6 mice for the *Apc*$^{+/+}$ and *Apc*$^{\Delta 14/+}$ genotypes. **B)** Kaplan-Meier plots of overall survival of patients with tumors exhibiting low or high RIP140 mRNA expression. **C)** RIP140 immunochemistry of a tissue microarray containing adenocarcinomas of 59 patients. Patients were ranked according to RIP140 expression in the tumor and divided into two groups exhibiting low and high RIP140 expression, respectively. A Kaplan-Meier plot of the cumulative survival of patients with low or high *RIP140* gene expression was performed. A log-rank test was used for statistical analysis. **D)** Schematic diagram picturing out the role of RIP140 on the β-catenin signaling in human colon cancer cells. RIP140 directly increases *APC* gene expression which inhibits activation of β-catenin (RIP140

reduces the levels of the unphosphorylated form of β-catenin). As a consequence of the drop in active β-catenin levels, RIP140 inhibits Wnt target gene expression and decreases the ability of human colon cancer cell to proliferate and form tumor in nude mice.